Assessment of post-contingency congestion risk of wind power with asset dynamic ratings

Banerjee, Binayak; Jayaweera, Dilan; Islam, Syed

DOI:
10.1016/j.ijepes.2014.12.088

Document Version
Peer reviewed version

Citation for published version (Harvard):
Banerjee, B, Jayaweera, D & Islam, S 2015, 'Assessment of post-contingency congestion risk of wind power with asset dynamic ratings', *International Journal of Electrical Power and Energy Systems*, vol. 69, pp. 295-303. https://doi.org/10.1016/j.ijepes.2014.12.088

Assessment of Post-Contingency Congestion Risk of Wind Power with Asset Dynamic Ratings

Binayak Banerjee[1] (corresponding author, email: binayak.banerjee@curtin.edu.au, tel. no. +61433581836),
Dilan Jayaweera[2] (email: D.Jayaweera@bham.ac.uk)
Syed Islam[1] (email: S.Islam@curtin.edu.au)

[1]Department of Electrical and Computer Engineering,
Curtin University, Kent Street, Bentley, Perth,
Western Australia 6102, Australia

[2]School of Electronic, Electrical and Systems Engineering
The University of Birmingham
Edgbaston, Birmingham, B15 2TT, UK

Abstract

Large scale integration of wind power can be deterred by congestion following an outage that results in constrained network capacity. Post outage congestion can be mitigated by the application of event control strategies; however they may not always benefit large wind farms. This paper investigates this problem in detail and proposes an advanced mathematical framework to model network congestion as functions of stochastic limits of network assets to capture post contingency risk of network congestion resulting through the constrained network capacity that limits high penetration of wind. The benefit of this approach is that it can limit the generation to be curtailed or re-dispatched by dynamically enhancing the network latent capacity in the event of outages or as per the need. The uniqueness of the proposed mathematical model is that it converts conventional thermal constraints to dynamic constraints by using a discretized stochastic penalty function with quadratic approximation of constraint relaxation penalty. The case study results with large and small network models suggest that the following an outage, wind utilization under dynamic line rating

can be increased considerably if the wind power producers maintain around a 15% margin of operation.

Keywords – dynamic asset ratings, locational marginal price, latent network capacity, stochastic optimization, wind power generation.

1. Nomenclature

$C_g(P_g)$	Cost of conventional generation
$C_w(P_w)$,	Cost of wind power feed in
C_{DLR}	Total cost of dynamic line rating
$C_{congestion}$	Total cost of network congestion
N_L	Total number of branches in network
N_k	Number of values in discretised probability distribution of line capacity
N_W	Total number of wind generators
$(h_{pq,k}, s_{max,pq,k})$	k^{th} Ordered pair (probability, value) representing line capacity probability distribution
$S_{sch,pq}$	Power flow in line from bus p to bus q
$a_{pq,k}$	The dynamic line capacity discrete probability distribution
c_{OLp}	Unit cost of dynamic line rating
$P_{local,n}$	Adjustment of load at bus n after redispatch during congestion
s_{jk}	Wasted wind discrete probability distribution
t_{jk}	Reserve requirement discrete probability distribution
c_D	Unit cost of network congestion
LMP_i	Locational Marginal Price at node i
$LMP_{i,base}$	Locational Marginal Price at node i during uncongested base case
P_W	Total wind power generation
$P_{W,base}$	Total wind power generation during uncongested base case
$P_{D,i}$	Real power demand at bus i
LMP_V	Index measuring variation in Locational Marginal Price from base case

2. Introduction

Network congestion is an undesirable result of insufficient capacity being available on a network to transport electricity from generation to loads. It leads to highly variable locational marginal prices (LMP) at nodes usually with high prices at load points which are affected by congestion compared to those which are not. A number of publications have used LMP as an indicator of network congestion [1-3]. In systems with large amount of wind power, network congestion hinders effective integration and utilization of wind as extra wind generated has to be curtailed thereby leading to uncertainty in revenue for wind power producers. The dynamic nature of wind results in large

variations in power output over a short period of time, which makes effective utilization of wind an even bigger challenge in congested networks.

Network congestion has a greater impact in networks under contingency. When a contingency occurs in a branch, the remaining branches in the network can experience greater loading and be at a higher risk of network congestion [4-7]. While traditional security analysis uses the N – 1 criterion this does not account for variation in output of wind leading to post contingency congestion and curtailment of wind. Therefore, even when a network seems to have no congestion and utilizes wind effectively, there is a high risk that any contingency will drastically change the situation.

A number of sources agree that the true thermal capacity of a transmission line is considerably higher than the rated values [8-12] since ratings are calculated under the worst case weather assumption although such operating conditions occurs rarely in practice. It is possible to exploit this property by using dynamic line ratings (DLR) which model the thermal limit of transmission lines as stochastically varying function of internal and external real time operating conditions such as ambient temperature, level of loading, intermittent effects, and sag. These methods capture real time variations and are an improvement over existing methods of using multiple thermal limits to account for different weather conditions based on the relationship between temperature and ampacity outlined in IEEE Std 738-2012 [13].

Some ISOs (independent system operators) currently use normal and emergency ratings as well as separate ratings for hot and cold weather. These ratings are an approximation of the real time variation in line ampacity and the actual thermal limit has a high likelihood of being significantly different. In modern power systems which consist of multiple competing entities and fast changing power flows due to presence of intermittent renewable generation, inaccurate estimation of real time ampacity can result in underutilization of network capacity and congestion. Dynamic ratings can provide a significant increase in the normal and emergency operational flexibility of power transmission systems compared to the more traditional static rating and alleviate network congestion due to short periods of high wind power output. DLR is applicable for power systems with short to medium lines where thermal capacity as opposed to stability limit is the limiting factor to line capacity.

The benefit of DLR over conventional congestion management approaches is that it can potentially release latent capacity dynamically rather than relying on generation curtailment and demand reduction in congested parts of a network, thus improving the operational flexibility and deferring investments. Dynamic line ratings can exploit the advanced real time monitoring and control capabilities of smart grids to potentially alleviate network congestion, and ensure a more equitable allocation of costs between market participants.

The two immediate challenges of implementing the dynamic line rating methods presented in [8-11] are the need for an online, smart monitoring system to capture real time variation and the modelling of uncertainty in constraints in optimal scheduling. While uncertainty in optimization variables can be accounted for by stochastic optimization techniques, uncertainty in constraints is more challenging to model since analytical constrained optimization techniques only allow fixed constraints. Most of the power system applications of optimal scheduling problems model line power transfer limits as deterministic values and place less emphasis on dynamic variation in line capacity. An alternative to this is chance constrained optimization which allows some flexibility in the constraint satisfaction by allowing constraint violation, provided their probability is limited to a specified value. [14, 15]

This paper proposes a new mathematical framework and a methodology to incorporate benefits of real time variation in line ratings to temporarily relax post-outage constrained capacity of a network and to vary reinforcement thresholds. The technique allows the stochastically estimated real time ampacity to be included in scheduling decisions by allowing a degree of flexibility to satisfy dynamic thermal limit constraints. The uniqueness of the proposed approach is that it replaces the current deterministic constraints (normal and emergency) in the optimal scheduling problem, with dynamic constraints. The approach dynamically quantifies the extent to which post outage constrained capacity could be relaxed by utilizing a discrete stochastic penalty function that takes into account the merits of dynamic line ratings. This method also incorporates the benefits of smart grid environments where real time data of system parameters such as sag and ambient temperature is available. The proposed approach could potentially provide considerable advantage over traditional approaches of using deterministic ratings due to the use of real time extraction of latent capacities during the optimization process. The paper also shows how dynamic line ratings can be used to reduce the risk of post outage network congestion while better facilitating wind integration for N – 1 and N – 2 contingencies. The proposed technique indicates the extent of congestion in a power network by weighting LMP at each node with respect to demand and finding the difference in the weighted LMP from the uncongested base case. The extended conic quadratic (ECQ) approach presented in [16] is used for optimization. It is modified to include dynamic line ratings.

3. Dynamic Asset Rating

3.1 Stochastic Optimisation with Dynamic Asset Ratings

The maximum thermal capacity of a line depends on the maximum allowable temperature of the line at which the conductors start to lose structural integrity or undergo annealing. IEEE Std 738 2012 outlines the process for calculating the maximum ampacity based on weather conditions for steady state, transient and dynamic scenarios. A number of models [8, 9, 11] apply the concepts in IEEE Std. 738 to determine dynamic line ratings which use weather data as an input. Kazerooni et al [10] have shown that when all the stochastic variations in weather are accounted for, the thermal capacity of the line can be modelled by the generalized extreme value probability distribution and in most cases the rated line capacity is on the lower end of the possible range of thermal capacities.

The correlation between wind speed and the cooling of the line was considered negligible in for this study, due the variation in weather conditions in different parts of a line [11]. While it is expected that weather conditions will mostly be favourable compared to the worst case assumptions for conventional line ratings, it is unlikely that all parts of the line will be exposed to high wind speeds which coincide with periods of high wind at the single location of the wind farm. It is assumed that the dynamic capacity is limited by regions where cooling due to wind is low and this provides a conservative estimate of the benefit due to DLR on wind integration. Typical parameters for the probability distribution of line capacity are provided in [10]. To determine the probability distribution of line ampacity historical weather data across the line will be necessary as per the procedure outlined in [10]. If correlation between wind speed and dynamic thermal ratings are to be accounted for, a different approach is required where the probability distribution of line capacity is conditional based on the probability of the wind speed distribution. A range of probability distributions for line capacity would be necessary for different wind speeds. Such an approach should be used with caution as it may overestimate the benefit of DLR.

The parameters of the probability distribution are determined according to the rated maximum limit on transmission lines. Based on the analysis in [8] most utilities load

their lines such that the probability of exceeding the rated capacity ranges from 20 – 30%, depending on the season. Thus it was assumed that the probability of exceeding the rated capacity was 25% and an inverse distribution was used to determine the parameters for the probability distribution. The probability distribution was discretised by considering ten frequency and value pairs to represent the probability distribution. The actual probability can vary depending on the utility but it is straightforward to perform the analysis with a different value. A more detailed study might treat this as a random variable. The objective function incorporating DLR as a penalty function with stochastic elements is shown in (1)

$$f(x) = C_g(P_g) + C_W(P_W) + C_{DLR} + C_{congestion} \quad (1)$$

where $C_g(P_g)$, $C_w(P_w)$, C_{DLR} and $C_{congestion}$ represent cost of conventional generation, cost of wind (including reserves), cost of dynamic ratings, and cost of congestion respectively. $C_g(P_g)$ and associated constraints of conventional OPF (optimal power flow) problems are given in [16-19]. $C_w(P_w)$ is the cost of uncertainty due to wind, which can be incorporated into OPF by using stochastic optimization and is given in [16]. The problem is solved by transforming to a conic quadratic optimization problem and using an interior point method [16, 20]. This has the advantage that the objective function becomes quadratic and almost all the constraints become linear. These transformations are not system dependent and hence can be applied directly without a modification.

3.2 Formulation

The total cost of DLR (C_{DLR}) in (1) is determined stochastically and represents the penalty for temporarily relaxing the line thermal constraint. The stochastic penalty function enables substitution of the static line thermal constraint with a dynamic constraint. The cost of DLR is partly due to the long term cost of derating due to repeatedly overloading lines and the short term risk of causing damage by severe overloading which causes line temperature to exceed the maximum allowable value. It is assumed that when implementing DLR, the short term risk and expected cost of thermal overload is considered much more significant than long term derating costs. Separate studies by Wang [21] and Zhang [22] describe the variation of thermal

overload risk with line current and demonstrate that for low levels of current overloading the risk of thermal overload is low but this increases rapidly for higher levels of DLR. Thus, the sensitivity of the penalty function to dynamic overloading must increase with increasing levels of DLR, thus suggesting an exponential penalty function. Instead it is modelled using a quadratic function as given in (2) since it can approximate the exponential function accurately for low levels of DLR, and the relative ease of calculating the Jacobian and Hessian matrices for quadratic functions.

$$C_{DLR} = \sum_{p=1}^{N_L} \sum_{q=1}^{N_L} \left[c_{OLp} \left(\sum_{k=1}^{N_k} h_{pq,k} a_{pq,k} \right)^2 \right] \tag{2}$$

where p-q represents a line from bus p to bus q. The cost of violating the constraint is proportional to the magnitude by which the actual line flow exceeds the line capacity. The constraints in (3) complement the expression for C_{DLR} in (2) to account for the cost of uncertainty in stochastic line rating.

$$\begin{aligned} a_{pq,k} &\geq s_{\max,pq,k} - S_{sch,pq} \\ a_{pq,k} &\geq 0 \end{aligned} \tag{3}$$

The thermal capacity of line p-q is approximated by a discrete random variable where each discrete value (represented by index k) of $s_{max,pq,k}$ has corresponding probability $h_{pq,k}$. The term $a_{pq,k}$ (with per unit cost c_{OLp}) represents the amount by which the actual line flow exceeds the discrete line capacity in the k^{th} ordered pair and it corrects any violation in the constraint $S_{sch,pq} > s_{max,pq,k}$. Thus ($h_{pq,k}$, $a_{pq,k}$) represents the probability distribution of dynamic line rating and the average value of $a_{pq,k}$ for all k represents the expected dynamic line rating.

The cost of DLR is based on the expected value of dynamic line rating which includes both the amount of DLR (a_{pq}) and the time for which it is implemented (h_{pq}). h_{pq} is an array of relative frequencies associated with each value of a_{pq}. If the time for which DLR is implemented varies, the value of $h_{pq,k}$ will change so that the probability distribution of a_{pq} changes. If the time for a specific amount of DLR is varied, it will change the probability distribution (specifically a change in probability for that level of DLR) and hence the expected value of DLR.

The DLR scheduling framework is to be used for a fixed scheduling period. This will typically be in the order of 15 – 30 minutes as longer periods of DLR will result in substantial risk of thermal overload. For the scheduling period under consideration,

DLR is implemented at all times or not at all and the risk of implementing DLR for that time is captured by the cost function. In practice, smart monitoring systems will record the line temperature at the start of the scheduling period and simulate the final line temperature at the end of the scheduling period including the uncertainty based on the method in IEEE Std. 738. Based on this, the probability of exceeding the maximum line temperature can be determined. The line capacity probability distribution for the given scheduling period can be determined by the generalized extreme value distribution and based on this capacity, current is scheduled to minimize the time for which the line is overloaded. The severity associated with an outage in the event that the risk of thermal overload is realized can be determined by the number of customers affected by the outage and the total energy not supplied.

The risk associated with thermal overload includes both the likelihood of exceeding line maximum temperature and the cost of an outage in the line under consideration. The value of c_{OLp} is chosen so that the quadratic function in (2) best fits the variation of risk of thermal overload with current. Thus the risk of thermal overload is described by the expected cost of outage in a particular line which is considered the cost/penalty of DLR. In the case studies, a number of different values of c_{OLp} are used to determine the effect that the cost of DLR has on the effectiveness of DLR.

The proposed approach assumes cost of congestion ($C_{congestion}$) to increase linearly with the extent of congestion in the system. The main contributor to $C_{congestion}$ is the cost of dispatching expensive reserve generation after lower cost generation has been curtailed. It is assumed that these rapid response reserve generators have minimal startup cost and a much smaller output range compared to large generators. They are distributed in the network and the operating cost over the small range of output is approximated by linear cost functions. Alternatively, load may have to be shed if redispatch cannot supply load. The penalty associated with shedding load is also assumed to be linearly related to the load curtailed as shown in (4).

$$C_{congestion} = \sum_{n=1}^{N} c_D P_{local,n} \tag{4}$$

s.t.

$$P_{local,n} \le P_{D,n},\ P_{local,n} \ge 0,$$

where $P_{local,n}$ represents any adjustment of load (by calling on local reserves or load shedding) at bus n (where the total number of buses is N). $P_{local,n}$ is required to balance

the system when congestion has occurred but it has a high cost per unit (c_D). Cost of network congestion can also represent the loss of revenue for generators since they cannot sell energy. This increased cost required to balance the system under congestion is allocated unevenly among customers which results in the volatility in nodal pricing that is observed during congestion.

For low levels of DLR, cost of congestion is higher relative to the risk of thermal overload from dynamically overloading lines. The optimization algorithm prefers to use DLR than call on expensive reserves after redispatch due to the lower cost of DLR. However, there is a maximum amount of DLR indicated by the intersection of the two functions in (2) and (4) beyond which, risk of DLR is greater than cost of congestion. Beyond the threshold point C_{DLR} is greater than $C_{congestion}$ thus forcing the optimization to not allow DLR beyond this limit as the risk associated with further overloading would not be justifiable. The DLR limit point represents both the maximum extent to which thermal limits can be relaxed and the time for which it can be relaxed

In addition to C_{DLR} and $C_{congestion}$ the basic OPF formulation includes generator fuel cost ($C_g(P_g)$) and constraints including real and reactive power balance, voltage limits, generator limits, and minimum generator up and down time. Line thermal constraints are replaced by the dynamic line rating formulation. The proposed approach modelled wind power intermittency cost ($C_w(P_w)$) using stochastic optimization by discretizing the probability distribution of wind power and balancing probabilistic reserve cost with cost of wasted wind [16] as shown in (5).

$$C_w(P_w) = \sum_{j=1}^{N_W} \left[e_j P_{Wj} + c_{Wj} \sum_{k=1}^{M} f_{jk} s_{jk} + c_{Rj} \sum_{k=1}^{M} f_{jk} t_{jk} \right] \tag{5}$$

Where the power output of wind generator j is P_{Wj} and the unit feed in cost is e_j. The cost of wind in (5) is subject to the constraints in (6).

$$\begin{aligned} t_{jk} &\geq P_{Wj} - w_{jk} \\ s_{jk} &\geq w_{jk} - P_{Wj} \\ t_{jk} &\geq 0, s_{jk} \geq 0 \end{aligned} \tag{6}$$

where (f_{jk}, w_{jk}) is the k^{th} ordered pair (out of a total of M) representing the discretized probability distribution of wind generator j. N_W is the number of wind generators in the system and c_{Wj} and c_{Rj} are the unit cost of wasted wind and reserve generation respectively at wind generator j. The cost of wasted wind represents the opportunity cost of not being able to sell the energy generated.

The problem was solved by transforming it to an extended conic quadratic (ECQ) form using the transformations in (7) [16, 20].

$$\begin{aligned} R_{in} &= V_i V_n \cos(\delta_i - \delta_n) \\ T_{in} &= V_i V_n \sin(\delta_i - \delta_n) \\ u_i &= \frac{V_i^{\,2}}{\sqrt{2}} \end{aligned} \tag{7}$$

Adding the rotated conic quadratic and arctangent equality constraints in (8) captured the nonlinearity of the classical OPF problem [16, 20].

$$\begin{aligned} 2u_i u_n &= R_{in}^{\,2} + T_{in}^{\,2} \\ \delta_i - \delta_n &= \tan^{-1}\left(\frac{T_{in}}{R_{in}}\right) \end{aligned} \tag{8}$$

All other constraints are transformed into linear expressions making the ECQ-OPF problem easily tractable by primal-dual interior point methods.

4. Case studies

The case studies are performed on the IEEE 14 bus test system and the IEEE 118 bus test system [23]. The wind speeds are generated by random numbers with a Weibull distribution and combined with the power speed characteristics of the turbines to obtain the wind power output. The wind farm locations, capacities, type of wind turbine and Weibull parameters are shown in Table 1. The power speed characteristics of the wind turbine were scaled to the capacity of the wind farm. At the specified wind farm locations, any existing conventional generation is replaced by equivalent amount of wind generation. The Weibull parameters are based on data obtained from the Albany and Emu Downs wind farms in Western Australia.

Table 1 Wind farm data

	Bus Number	***Rated capacity (MW)***	***Weibull parameters (c,k)***	***Wind turbines power curve***
14 bus	6	100	(7.2, 2.35)	Enercon E66
	8	30	(7.8, 2.80)	Vestas V82
118 bus	12	85	(7.2, 2.35)	Enercon E66
	25	220	(7.8, 2.80)	Vestas V82
	59	155	(7.3, 2.41)	Enercon E66
	80	477	(7.7, 2.77)	Vestas V82

Buses 6 and 8 in the standard IEEE 14 bus system have synchronous condensers with no active power injection. Connecting wind turbines to these buses will provide active power injection with necessary reactive power support for wind turbines from the synchronous condensers. In the 118 bus system the choice of wind farm buses were based on a number of factors such as dispersion of wind farms throughout the grid, ensuring there were wind farms of different capacities and to ensure the overall wind capacity available was adequately high so that the effects of congestion were observable.

The GEV distribution describing the dynamic line capacity is characterized by the mean, shape parameter and scale parameter. Typically, when a line is operating at nominal capacity, the probability of the nominal capacity underestimating the true capacity ranges from 70 – 80% [8]. Thus, the probability of underestimating the true capacity was assumed to be 75% and an inverse distribution was used to determine the mean for the probability distribution. The shape and scale parameters were set to -0.2 and 0.03 respectively which are typical values [10, 24]. By varying the mean, shape and scale parameters, the extent of DLR capability in a line can be controlled. A more detailed study might consider the probability of line overload to be varying in real time. Both the systems are compared in terms of LMP profile and wind curtailment for a number of outages with and without DLR. Risk profiles with and without DLR are also compared for both systems in addition to the effect on generation mix during congestion

Risk of network congestion is the product of likelihood and the severity of network congestion. The severity of congestion is indicated by the volatility in LMP and the amount of wind curtailment. Volatility in LMP is most commonly used as an indicator of network congestion as congestion cost is a significant component of LMP in transmission systems [2, 3, 25]. Pricing signals have been proposed as a control mechanism for renewable energy integration [26]. The proposed method first establishes a base case for LMP without incorporating network constraints. For each outage scenario, the LMP at each bus is compared to the base case LMP, weighted by the load at that bus and the overall weighted variation in LMP is found. To compare the LMP profile of a specific case to the base case, the term LMP_V is defined by (9).

$$LMP_V = \sqrt{\frac{1}{\sum_{i=1} P_{D,i}} \left(\sum_{i=1} \left[P_{D,i} \left(\frac{LMP_i - LMP_{i,base}}{LMP_{i,base}} \right)^2 \right] \right)} \tag{9}$$

LMP_V is the LMP normalized by base LMP and has no units. A large value of LMP_V generally indicates that the given LMP profile is very different to the uncongested LMP profile which most likely suggests that the network is congested.

The likelihood of network congestion is determined from the probability of the outages which lead to network congestion. Likelihood of N – 1 outages are determined directly from the probability of failure of a specific line. Likelihood of N – 2 outages are determined as the probability of two independent N – 1 outages or as a common mode outage where one event causes multiple outages.

Wind curtailment is normalized with respect to the wind generation in the uncongested base case and determined by (10).

$$\text{wind curtailed} = \frac{P_{w,base} - P_w}{P_{w,base}} \tag{10}$$

The spare capacity in the network is measured as the total available capacity expressed relative to the total rated capacity of all lines and is determined by equation (11).

$$\text{spare capacity} = \frac{\sum_{all\ lines} (I_{\max} - I_{flow})}{\sum_{all\ lines} I_{\max}} \tag{11}$$

Where I_{max} is the magnitude of maximum current in a line and I_{flow} is the magnitude of current actually flowing in the line. In the case studies, additional spare capacity required to relieve network congestion is used to determine the capacity released by DLR.

4.1 Modified IEEE 14 bus system

The first test established the base case scenario, without any contingency in the system with LMP profile shown in Fig. 1(a).

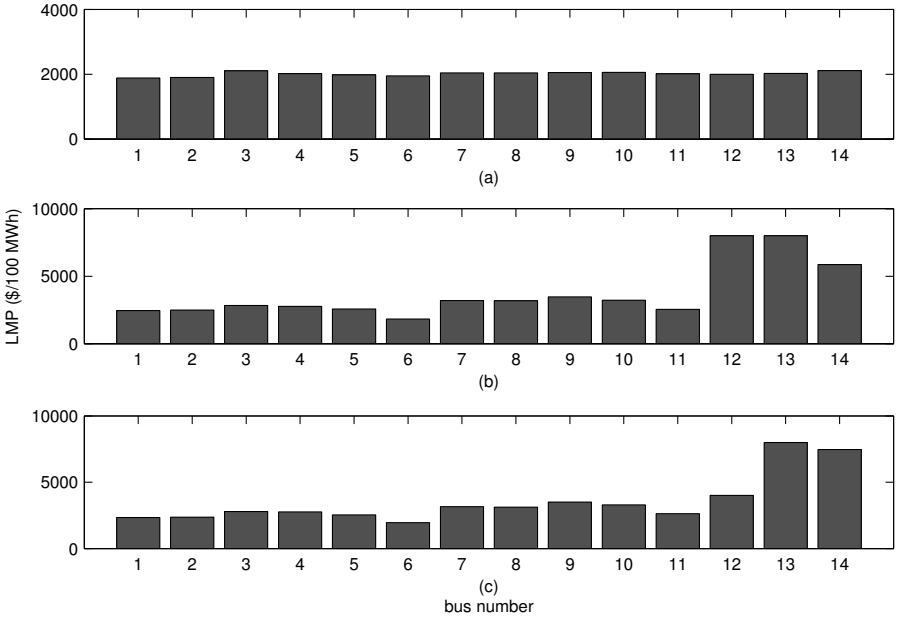

Fig. 1 LMP profile (a) before congestion, base case (b) Line 6-12 removed (c) Line 6-12 removed but with dynamic asset rating

Fig. 1 (a) shows minimum variation in LMP indicating no congestion. Fig. 1(b) shows the effect of an outage in line 6-12 on the LMP profile which shows a significant rise in LMP in nodes 12, 13 and 14. Fig. 1(c) shows that DLR reduces the LMP in node 12 thereby reducing network congestion but not eliminating it completely.

Fig. 2 shows the line percentage loading profiles. Fig. 2(a) shows the line loading profile for the network under normal conditions (without any contingencies). Under normal operating conditions, all the lines connected to wind farm 1 are loaded to 85% - 98% of full capacity.

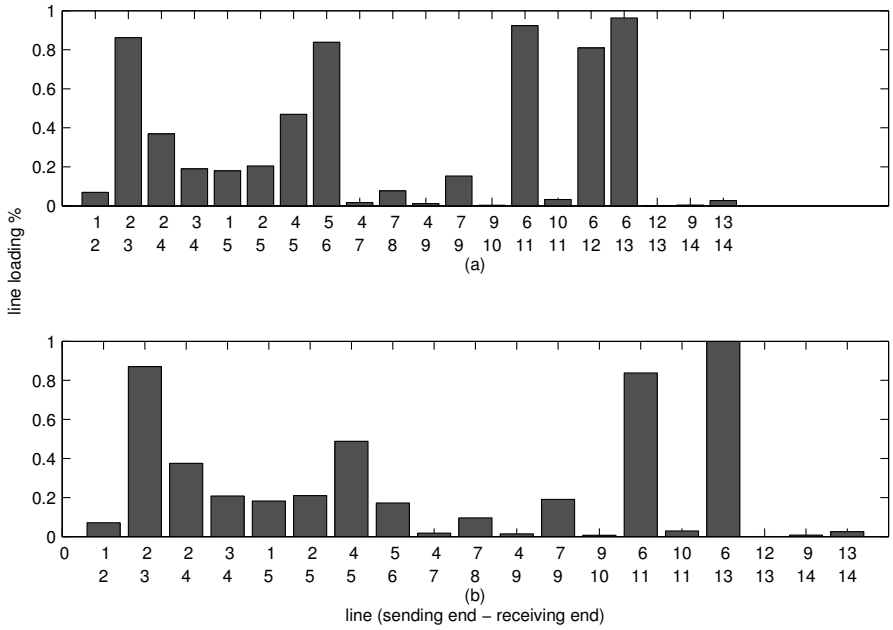

Fig. 2 Line loading percentage (a) base case (b) after outage in line 6 – 12.

After an outage, line 6 – 13 is at 100% capacity (Fig. 2(b)) and congestion results as seen in Fig. 1(b). The spare capacity is measured as the total available capacity expressed relative to the total rated capacity of all lines and is determined by equation (11).

$$spare\ capacity = \frac{\sum_{critical\ \ lines} (I_{\max} - I_{flow})}{\sum_{critical\ \ lines} I_{\max}} \qquad (6)$$

Where I_{max} is the magnitude of maximum current in a line and I_{flow} is the magnitude of current actually flowing in the line. Spare capacity is calculated for all the critical lines in the system which are identified as those connected directly to bus 6 (the wind bus). These are defined as critical lines because these lines are loaded close to their full capacity and likely to be congested in the event of contingencies.

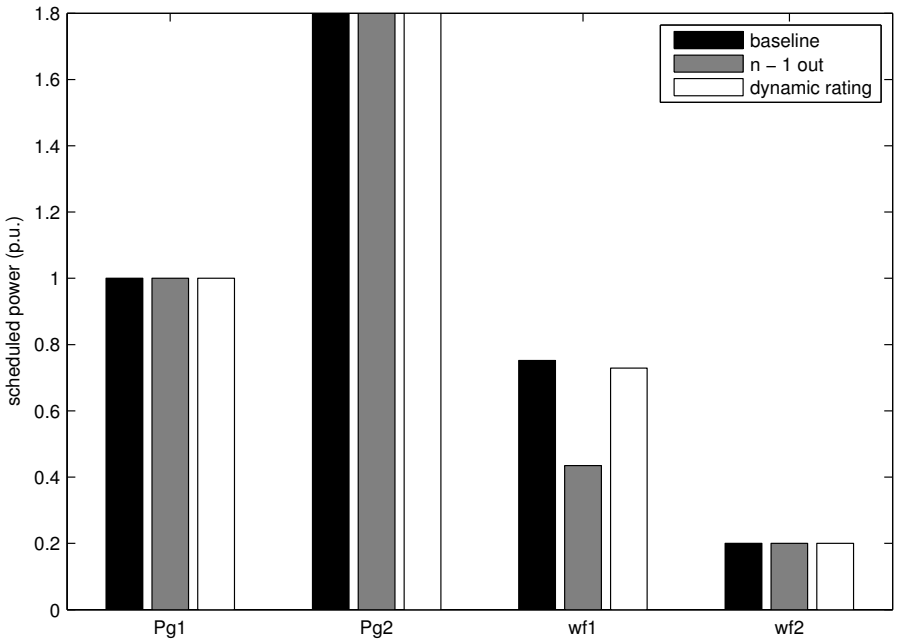

Fig. 3 Generation mix under different conditions

Fig. 3 shows the generation mix which indicates curtailment of wind as a result of congestion. The output of wf1 is curtailed when the line 6 – 13 experiences an outage. When the dynamic rating of assets is considered it restores the scheduled wind output to the pre contingency value. In this case, if the DLR is incorporated for the assessment/ decision-making process then the post-contingency impact on wind farm output can be eliminated.

Wf2 is not affected by the contingency because the congestion is localized to wf1. The wind curtailed is normalized with respect to the wind generation in the uncongested base case and determined by equation (10).

$$wind\,curtailed = \frac{P_{w,base} - P_{w}}{P_{w,base}} \tag{7}$$

Table 2 summarizes the effect of different outages on the system. Only outages resulting in significant congestion are reported in Table 2.

Table 2 Comparison of Congestion with and without DLR

Case No.	line out	*No DLR*		*with DLR*		spare capacity required to match DLR
		LMP variation	wind curtailed	LMP variation	wind curtailed	
1	none	0.0	0%	0.0	0%	-
2	6-11	6.07	8%	2.21	1%	18%
3	6-12	5.07	13%	0.52	1%	22%
4	6-13	8.05	33%	4.54	2%	54%
5	6-11, 6-12	6.52	23%	2.81	2%	26%
6	12-13, 6-13	6.87	34%	4.09	8%	27%
7	13-14, 6-12	6.20	14%	2.37	1%	24%
8	12-14, 6-13	7.50	33%	4.04	5%	44%

It is seen that DLR reduces congestion (although doesn't eliminate it completely) and reduces wind curtailment. The line loading is shown as a percentage of line capacity for each line in Fig. 4. When outages in critical lines are considered, the reduction in average $LMP_{variation}$ ranges between 43 – 64%, with exceptional cases of being as high as 89% (case 3). Congestion in a line is not always due to physical thermal limits. In some cases the line may not be at the thermal limit, but further power flow through the lines would cause voltage drops that would violate constraints. As a result the flow through the line is limited. This is the reason why DLR cannot completely eliminate congestion. In cases where non critical lines with low levels of loading experience an outage, the increase in $LMP_{variation}$ would be negligible and dynamic line rating would have limited effectiveness.

For comparison, Table 2 presents the amount of spare capacity that would be required to reduce congestion to the same level as DLR. Thus, dynamic asset rating can allow the cost of network reinforcement to be deferred. In the presented cases, if a worst case scenario design were to be carried out, then 54% of spare capacity would have to be built into the system to provide the same benefit as DLR (outage of line 6 – 13 as per case 4).

Table 2 also showed that while some N – 2 outages lead to higher value of $LMP_{variation}$ compared to the corresponding N – 1 outage this is not always the case. For example when 6 – 13 is out (N – 1) $LMP_{variation}$ is 7.3% higher than when 12-14 is also out. While this would initially indicate a higher level of congestion with the N – 1 outage as opposed to the n-2 outage a closer examination of the LMP profile is required. Fig. 4 shows the LMP profiles of an (N – 1) outage (case 4) and an (N – 2) outage (case 8).

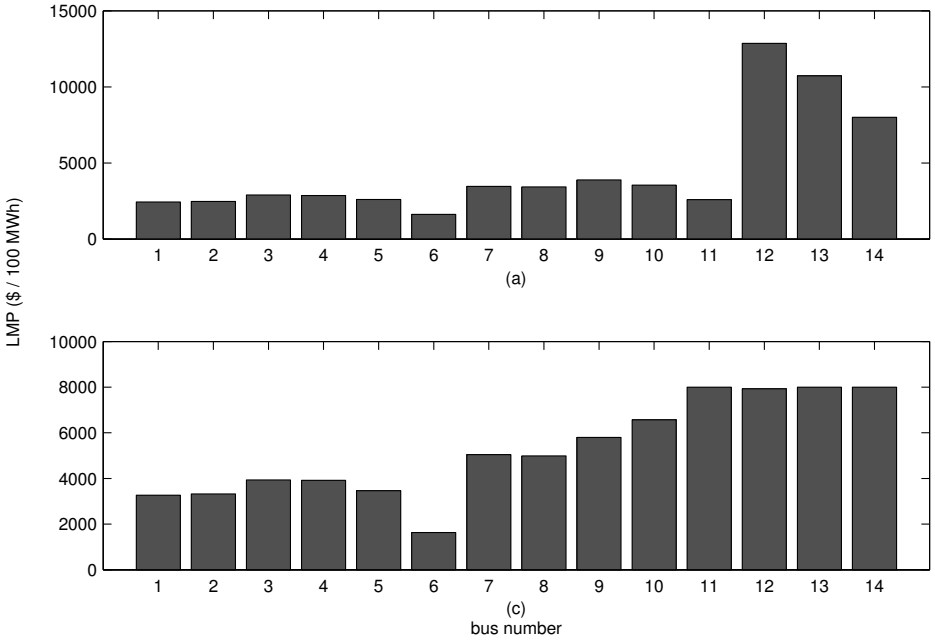

Fig. 4 Comparison of LMP profiles (a) line 6-13 out (N-1) (b) lines 12-14 and 6-13 out (N-2)

While the LMP profile in Fig. 4(a) is generally flatter, the three nodes (12, 13, 14) with a higher LMP skews the average LMP variation. In Fig. 4(b) the average difference to the base line case may be smaller but more nodes have a higher price than the base case. So the N – 2 outage leads to higher LMP in more buses even though the increase in LMP per bus is lower than the N – 1 case.

4.2 Modified IEEE 118 bus system

The envelope of a number of sample LMP profiles for different values of LMP_V for the IEEE 118 bus system is shown in Fig. 5. There is a slight visible congestion at LMP_V =

0.165 since nodes 90 and 91 have a higher LMP than the base case, as indicated in Fig. 5. Below 0.165 there is no discernible change in LMP and hence for the remaining case studies LMP_V less than 0.165 is considered insignificant.

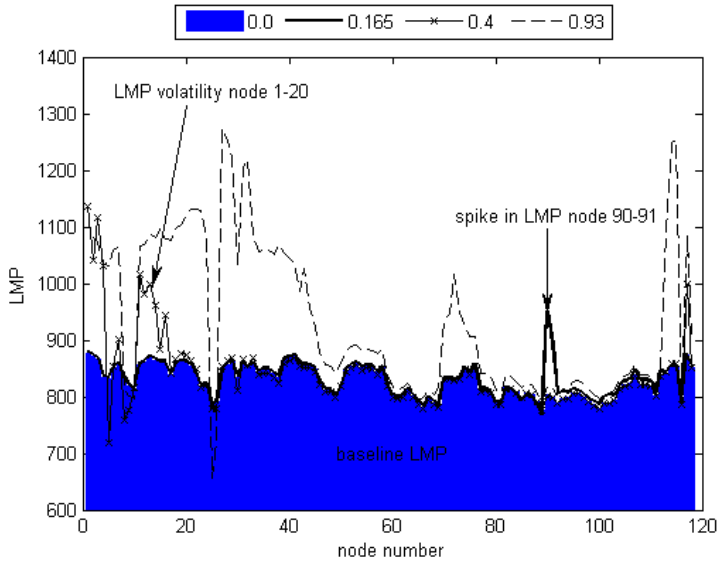

Fig. 5 Comparison of baseline LMP distribution and LMP distribution envelopes for LMP_V = 0.165, 0.4, and 0.93 in IEEE 118 bus system

Fig. 8 shows the risk profile and histogram of outages with significant congestion out of 150 simulated cases. In addition to independent N – 2 and N – 1 outages common mode outages were also considered. According to Fig. 8 (b) for the IEEE 118 bus test system only 50% of the outages resulted in severe congestion as compared to 95% of outages for the IEEE 14 bus test system. This is because for a large system with the generation more dispersed, there are many options for redispatch so not all outages lead to severe congestion. The range of LMP_V following an outage without DLR is 0.165 to 30 with the most of the outages resulting in an LMP_V of 13-18. After DLR has been implemented following an outage, LMP_V with DLR has a range of 0 to 17 with most outages having very low LMP_V.

Fig. 7 shows the wind curtailment profile for the 118 bus system. In a worst case scenario using DLR reduces the wind curtailment from 20% to 5%. In approximately half the simulated outages the wind curtailment (both with and without DLR) is negative indicating that wind integration increases after an outage. This is unexpected and since it occurs in a third of all the cases an examination of the wind generation profile for two sample outages with negative wind curtailment is undertaken in Fig. 9.

In Fig. 9 (a) there is an outage in branch 23 – 25 resulting in 5% increase in wind integration after the outage and without DLR. The wind power output of bus 12, 25 and to a lesser extent bus 59 increases after the outage since there is inadequate conventional generation. When DLR is implemented wind farm output on buses 12 and 25 decreases slightly as DLR has made more conventional generation available; however not as much as before the outage occurred. This is due to the varying levels of DLR in different branches. DLR results in slightly more wind integration on bus 59 as it is likely that there is greater DLR capability in the surrounding network. The wind farm on bus 80 is at maximum capacity and is unaffected by the outages and DLR. The value of LMP_V is 0.8 without DLR and 0.6 with DLR which is relatively low.

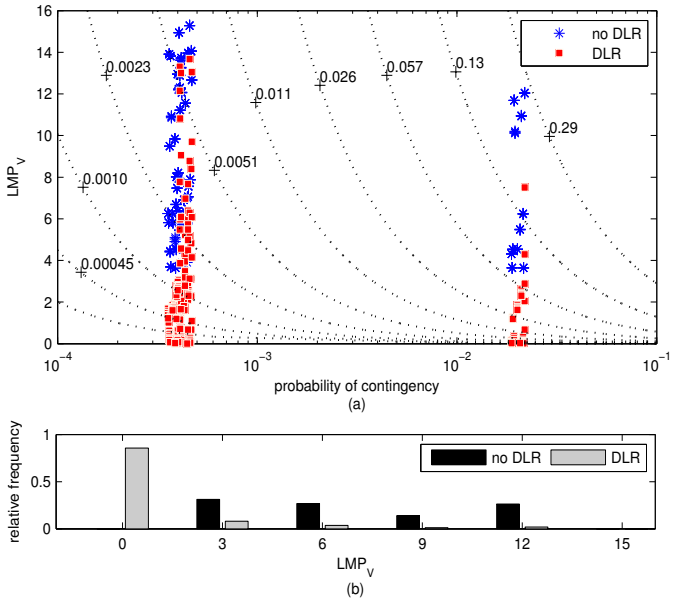

Fig. 6 Comparison of post outage risk profile of 14 bus system with and without DLR (a) outages against risk contours (b) histogram of LMP_V

Fig. 9 (b) shows the wind power generation for the outage of branches 63 – 65 and 38 – 65. After the outage there is a 15.3% increase in wind penetration. Wind generators on buses 12, 25 and 59 increase their output after the outage and wind generator on bus 80 is curtailed. The loss of the two branches leads to loss of major channels to transfer power generated at bus 80. As a result wind generation at bus 80 is curtailed and other wind generators have the opportunity to increase their output proportionally. Pre DLR LMP_V is 32 and this reduces to 4.7 post DLR when the output of bus 80 increases to pre outage levels. However, due to the variable extent of DLR in different sections the

outputs of other wind generators do not reduce proportionally.

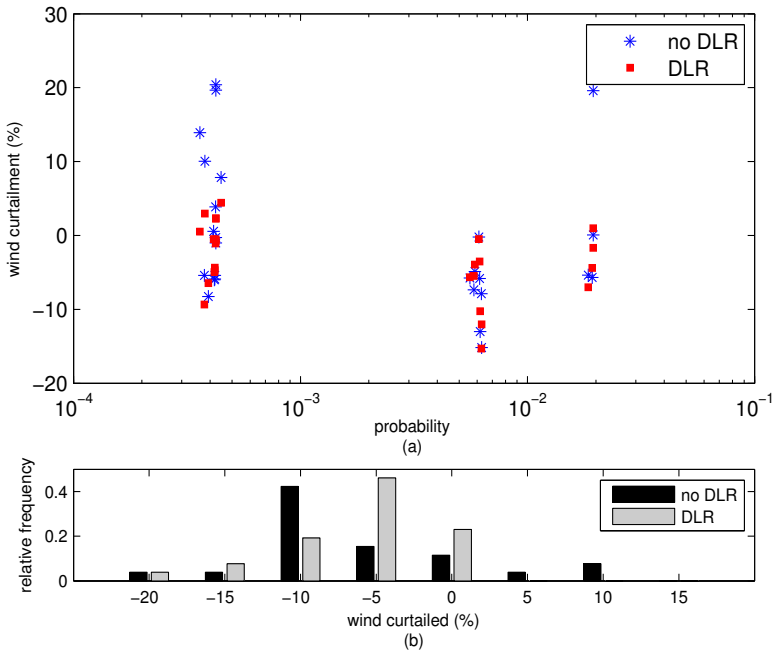

Fig. 7 (a) Post outage wind curtailment profile for 118 bus system (b) Histogram of post outage wind curtailment

The phenomenon of increased wind integration after an outage is a result of congestion limiting conventional generator output which provides wind farms the opportunity to increase their output provided they have enough reserves available. Implementing DLR may further increase capacity around wind farms thus increasing their output further.

The effect of unit DLR cost on the reduction in congestion is shown in Fig. 10. Fig. 10 (a) shows the variation in the boxplot of LMP_V for different values of c_{OLp}. A lower value of c_{OLp} leads to a narrow interquartile range of LMP_V and a lower median. Both of these parameters increase as c_{OLp} increases and effectiveness of DLR reduces. At the highest tested value of c_{OLp} (3000) the boxplot is almost identical to the no DLR case. Fig. 10 (b) shows the variation in mean value of LMP_V which increases as c_{OLp} increases. When c_{OLp} is 3000 the mean LMP_V is almost equal to the LMP_V without DLR implemented. This is the threshold at which DLR becomes completely ineffective.

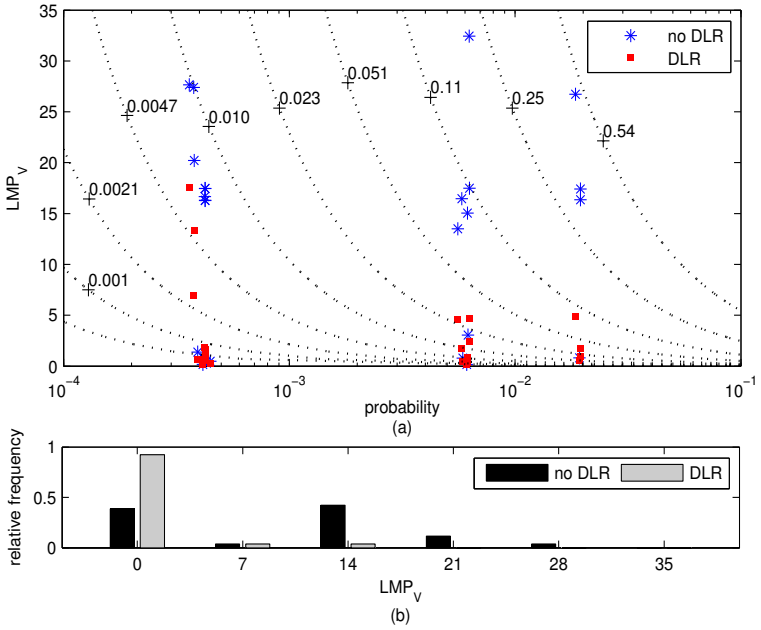

Fig. 8 Comparison of post outage risk profile of 118 bus system with and without DLR (a) outages against risk contours (b) histogram of LMP_V

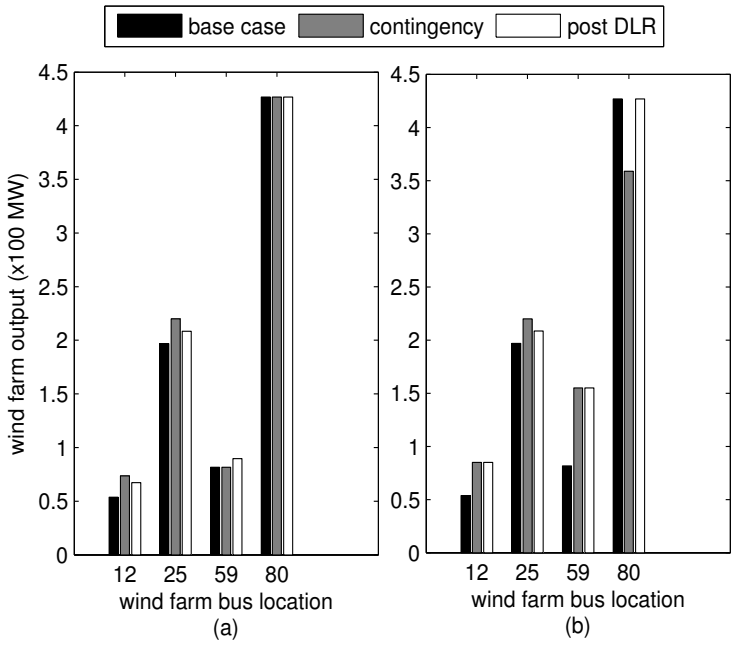

Fig. 9 Wind power generation profile for outage in (a) branch between bus 23 – 25 (b) branches between bus 64 – 65 and 38 – 65

The relationship between c_{OLp} and congestion cost is shown in Fig. 11 for different values of c_{OLp}. The value next to each curve represents the value of c_{OLp} for that curve. The relationship between cost of DLR and the cost of network congestion influences the effectiveness of DLR. DLR cost is lower than the cost of congestion for low levels of DLR. However, depending on the shape of the cost curve, DLR cost will exceed the cost of congestion for a certain level of DLR. The intersection of the DLR cost and congestion cost determines the threshold cost beyond which DLR will be ineffective for a given system. The threshold DLR decreases as c_{OLp} increases. When c_{OLp} is 3000 the maximum possible amount of DLR is insufficient to allow enough power flows to alleviate congestion. As a result, DLR provides no benefit in reducing congestion and the mean LMP_V is almost equal to the mean LMP_V with no DLR.

The cost of DLR not only reflects the long term cost of repeatedly overloading the line but also the attitude of the system operator in terms of the amount of risk that is considered acceptable. In an extreme case a system operator may assume that there is no tangible cost in the short term and allocate a very low cost to DLR because alleviating network congestion is an immediate priority. On the other side of the spectrum the network operator may decide that the risk associated with temporarily overloading lines is too great and allocate a high cost thereby reducing the effectiveness of DLR. Ideally, the network operator should consider the severity and risk of congestion and weigh this against the risk associated with DLR. The risk associated with DLR also includes the risk to system security and reliability if thermal ratings are completely relaxed. The cost function should be chosen such that the thermal constraints are not fully relaxed at any time. If there are specific instances when implementing DLR could increase the risk to system security to unacceptable levels (as deemed by the system operator) then the cost function can be adjusted so that the DLR threshold point reduces the maximum allowable amount of DLR. The cost of DLR is not necessarily constant and it is expected that depending on priorities at any given time it will be varied.

Table 3 Comparison of Congestion with and without DLR For 118 bus system

No.	***Branch out***	***No DLR***		***DLR***		***Spare capacity***
		LMP_V	***WC %***	***LMP_V***	***WC %***	
1	23-25	17.4	19.5	0.93	0.97	6.79 / 13.1

2	23-25, 25-27	20.2	10.0	13.3	2.97	13.8 / 19.4
3	23-25, 81-80	17.4	19.6	0.91	2.25	6.93 / 11.1
4	26-25, 25-27	16.4	- 7.35	1.70	- 5.49	5.38 / 3.51
5	25-27	16.4	0.05	1.72	- 1.67	5.02 / 8.63
6	25-27, 26-30	27.6	13.9	17.56	0.52	10.2 / 19.7
7	25-27, 77-80	16.7	3.88	1.81	- 1.08	4.88 / 14.6
8	25-27, 81-80	16.3	1.03	1.64	0.51	5.05 / 3.71
9	26-30	26.7	- 5.38	4.87	- 7.01	8.52 / -
10	26-30, 8-30	27.4	- 5.40	6.90	- 9.33	8.32 / -
11	38-65, 64-65	32.4	- 7.88	4.67	- 15.3	4.89 / 4.89

WC = wind curtailed
Spare capacity = % extra capacity required to match DLR (congestion/ wind curtailment)

Table 3 shows the minimum spare capacity required as calculated by (11) required to match the effect of DLR for selected cases. These scenarios were chosen as they have the highest congestion out of all the simulated cases. The minimum capacity expansion which reduces LMP_V to post DLR levels does not necessarily reduce wind curtailment to post DLR levels. Further capacity expansion is required to reduce wind curtailment to be comparable with the post DLR case. In some scenarios (case 9 and 10) no amount of capacity expansion leads to the wind curtailment being as low as in the DLR case. The minimum additional capacity required quantifies the latent capacity that DLR can release at a fraction of the cost of network upgrade. Network upgrade projects are often expensive and not justifiable for low likelihood outages causing network congestion. Dynamic line rating would reduce severity of these outages at a fraction of the cost and increase overall network robustness. To gain maximum benefit from capacity expansion it must be targeted at bottleneck regions. It is likely that if all the scenarios were to be covered, the real amount of capacity expansion would be much larger as most outages are in different parts of the network.

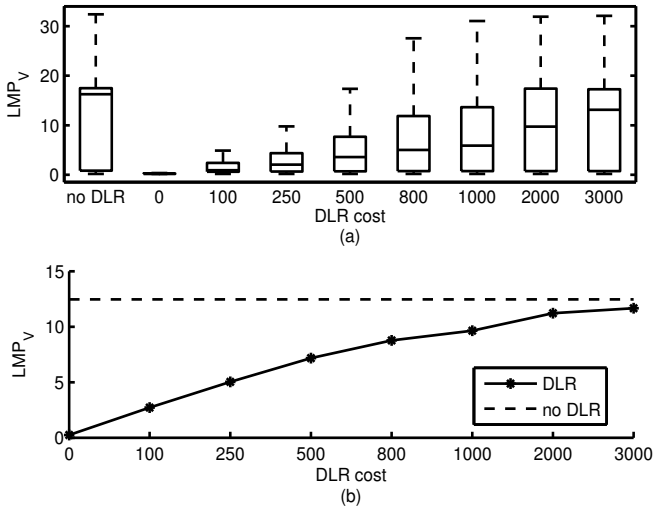

Fig. 10 (a) Boxplot of LMP_V versus different levels of DLR cost (b) Variation of mean LMP_V with DLR cost.

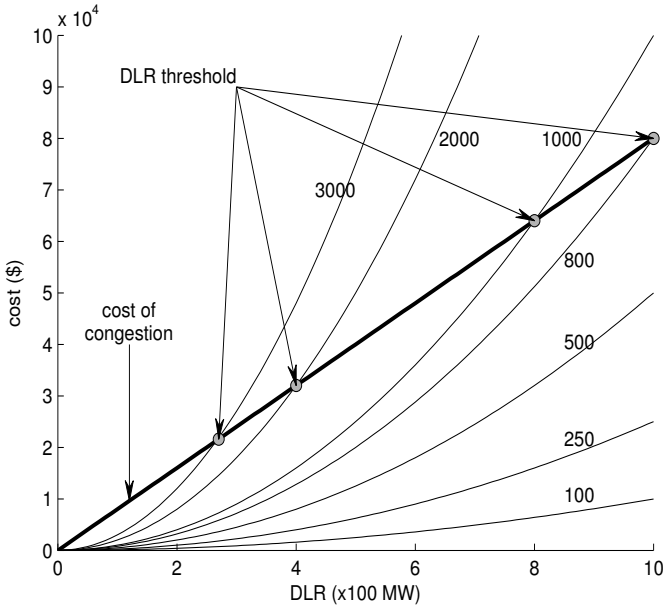

Fig. 11 Comparison of DLR cost to congestion cost for different levels of DLR cost

In the event of outages with negative wind curtailment there is an opportunity for wind power producers to provide emergency generation and increase their revenue. Given that a third of the simulated cases resulted in increased wind integration after an outage,

it is worth assessing the likelihood and potential cost versus benefit of such outages when sizing storage and reserves. The wind power producers may have an agreement where they will be remunerated at a higher rate if they maintain the extra reserve margin to provide emergency support. The factors which determine whether an outage results in negative curtailment are the location of the outage, the extent of DLR capability of each line and the location of conventional generation relative to wind generation.

The method proposed for modelling real time variation in line rating will be practical within the context of a smart grid since is expected that infrastructure to monitor ambient temperature, wind speeds, and line sag in real time in multiple locations will be readily available. This information will be utilized by the system operator to update the line rating and dispatch as frequently as necessary. Another important consideration when implementing DLR is the operation of protection systems including over current relays which may operate if thermal limits are exceeded. Smart protection devices will be necessary to ensure that the protection system can distinguish between overcurrent and DLR events. Distance protection may be a practical solution as DLR will not lead to a significant change in voltage as in the case of a fault. Alternatively, protection devices which directly monitor line temperature and operate when there is considerable risk of thermal overload may be used instead of overcurrent relays.

Implementing DLR in a smart grid also has the advantage that system security and reliability can be monitored in real time. In some cases system security and reliability may be compromised if DLR is implemented. The smart grid infrastructure should not allow DLR in such conditions. One method of implementing this would be to use the information to update the cost function of DLR in real time so that the maximum allowable extent of DLR is reduced.

5. Conclusion

The paper proposed a new mathematical framework to assess the potential ability of DLR to reduce risk of network congestion by limiting the curtailment levels of wind power in power systems. Case studies suggest that DLR can potentially release a considerable amount of capacity of network assets, enabling increased wind power integration. Wind integration under N – 1 and N – 2 outages can increase further if wind power producers maintain around a 15% margin of operation. The resulting margin of

operation is used to provide standing reserve while reducing the stress by DLR operation.

Power systems need periodic investment planning to meet growth in demand, uncertainties, and risks associated with active operation. In that context, the proposed approach can be used to monitor the net network reinforcement requirement in power systems by utilizing the benefits that can be offered by DLR of assets under normal operation and credible outages.

6. References

[1] M. Khanabadi, H. Ghasemi, Transmission congestion management through optimal transmission switching, in: Power and Energy Society General Meeting, 2011 IEEE, 2011, pp. 1-5.

[2] K. Shaloudegi, N. Madinehi, S.H. Hosseinian, H.A. Abyaneh, A Novel Policy for Locational Marginal Price Calculation in Distribution Systems Based on Loss Reduction Allocation Using Game Theory, Power Systems, IEEE Transactions on, 27 (2012) 811-820.

[3] K. Singh, N.P. Padhy, J. Sharma, Influence of Price Responsive Demand Shifting Bidding on Congestion and LMP in Pool-Based Day-Ahead Electricity Markets, Power Systems, IEEE Transactions on, 26 (2011) 886-896.

[4] M.A. Rahim, I. Musirin, I.Z. Abidin, M.M. Othman, Contingency based congestion management and cost minimization using bee colony optimization technique, in: Power and Energy (PECon), 2010 IEEE International Conference on, 2010, pp. 891-896.

[5] Z. Xiaosong, L. Xianjue, P. Zhiwei, Congestion management ensuring voltage stability under multicontingency with preventive and corrective controls, in: Power and Energy Society General Meeting - Conversion and Delivery of Electrical Energy in the 21st Century, 2008 IEEE, 2008, pp. 1-8.

[6] C. Thompson, K. McIntyre, S. Nuthalapati, A. Garcia, E.A. Villanueva, Real-time contingency analysis methods to mitigate congestion in the ercot region, in: Power & Energy Society General Meeting, 2009. PES '09. IEEE, 2009, pp. 1-7.

[7] J.D. Lyon, K.W. Hedman, M. Zhang, Reserve Requirements to Efficiently Manage Intra-Zonal Congestion, Power Systems, IEEE Transactions on, PP (2013) 1-8.

[8] J. Fu, D.J. Morrow, S. Abdelkader, B. Fox, Impact of Dynamic Line Rating on Power Systems, Universities' Power Engineering Conference (UPEC), Proceedings of 2011 46th International, (2011) 1-5.

[9] J. Hosek, P. Musilek, E. Lozowski, P. Pytlak, Effect of time resolution of meteorological inputs on dynamic thermal rating calculations, Generation, Transmission & Distribution, IET, 5 (2011) 941-947.

[10] A.K. Kazerooni, J. Mutale, M. Perry, S. Venkatesan, D. Morrice, Dynamic thermal rating application to facilitate wind energy integration, in: PowerTech, 2011 IEEE Trondheim, 2011, pp. 1-7.

[11] M. Matus, D. Saez, M. Favley, C. Suazo-Martinez, J. Moya, G. Jimenez-Estevez, R. Palma-Behnke, G. Olguin, P. Jorquera, Identification of Critical Spans for Monitoring Systems in Dynamic Thermal Rating, Power Delivery, IEEE Transactions on, 27 (2012) 1002-1009.

[12] Y. Yi, R.G. Harley, D. Divan, T.G. Habetler, Thermal modeling and real time overload capacity prediction of overhead power lines, in: Diagnostics for Electric Machines, Power Electronics and Drives, 2009. SDEMPED 2009. IEEE International Symposium on, 2009, pp. 1-7.

[13] IEEE Standard for Calculating the Current-Temperature Relationship of Bare Overhead Conductors, IEEE Std 738-2012 (Revision of IEEE Std 738-2006 - Incorporates IEEE Std 738-2012 Cor 1-2013), (2013) 1-72.

[14] Z. Hui, L. Pu, Chance Constrained Programming for Optimal Power Flow Under Uncertainty, Power Systems, IEEE Transactions on, 26 (2011) 2417-2424.

[15] W. Qianfan, G. Yongpei, W. Jianhui, A Chance-Constrained Two-Stage Stochastic Program for Unit Commitment With Uncertain Wind Power Output, Power Systems, IEEE Transactions on, 27 (2012) 206-215.

[16] R.A. Jabr, B.C. Pal, Intermittent wind generation in optimal power flow dispatching, Generation, Transmission & Distribution, IET, 3 (2009) 66-74.
[17] G.L. Torres, V.H. Quintana, An interior-point method for nonlinear optimal power flow using voltage rectangular coordinates, Power Systems, IEEE Transactions on, 13 (1998) 1211-1218.
[18] X.P. Zhang, S.G. Petoussis, K.R. Godfrey, Nonlinear interior-point optimal power flow method based on a current mismatch formulation, Generation, Transmission and Distribution, IEE Proceedings-, 152 (2005) 795-805.
[19] L. Shi, C. Wang, L. Yao, Y. Ni, M. Bazargan, Optimal Power Flow Solution Incorporating Wind Power, Systems Journal, IEEE, 6 (2012) 233-241.
[20] R.A. Jabr, Optimal Power Flow Using an Extended Conic Quadratic Formulation, Power Systems, IEEE Transactions on, 23 (2008) 1000-1008.
[21] W. Kongsen, S. Gehao, J. Xiuchen, Risk assessment of transmission dynamic line rating based on Monte Carlo, in: Power Engineering and Automation Conference (PEAM), 2011 IEEE, 2011, pp. 398-402.
[22] Z. Jun, P. Jian, J.D. McCalley, H. Stern, W.A. Gallus, Jr., A Bayesian approach for short-term transmission line thermal overload risk assessment, Power Delivery, IEEE Transactions on, 17 (2002) 770-778.
[23] U.o. Washington, Power Systems Test Case Archive, in, University of Washington, 1993.
[24] B. Banerjee, D. Jayaweera, S.M. Islam, Probabilistic optimisation of generation scheduling considering wind power output and stochastic line capacity, in: Universities Power Engineering Conference (AUPEC), 2012 22nd Australasian, 2012, pp. 1-6.
[25] Z. Qun, L. Tesfatsion, L. Chen-Ching, Short-Term Congestion Forecasting in Wholesale Power Markets, Power Systems, IEEE Transactions on, 26 (2011) 2185-2196.
[26] G.T. Heydt, B.H. Chowdhury, M.L. Crow, D. Haughton, B.D. Kiefer, M. Fanjun, B.R. Sathyanarayana, Pricing and Control in the Next Generation Power Distribution System, Smart Grid, IEEE Transactions on, 3 (2012) 907-914.